Magnon specific heat of single-crystal borocarbides $R\mathrm{Ni_2B_2C}$ (R=Tm, Er, Ho, Dy, Tb, Gd)

M. El Massalami, R. E. Rapp, and F. A. B. Chaves
Instituto de Fisica-UFRJ, Caixa Postal 68528, 21945-970 Rio de Janeiro, Brazil

H. Takeya
National Institute for Materials Science, 1-2-1 Sengen, Tsukuba, Ibaraki 305-0047, Japan

C. M. Chaves
Departamento de Fisica, PUC-Rio, 22453-900 Rio de Janeiro, Brazil

(Received 2 October 2001; revised manuscript received 25 February 2003; published 10 June 2003)

Zero-field specific heats of the single crystals $R\mathrm{Ni_2B_2C}$ (R=Er, Ho, Dy, Tb, Gd) were measured within the temperature range 0.1 K$<T<$25 K. Linearized spin-wave analysis was successfully applied to account for and to rationalize the thermal evolution of the low-temperature magnetic specific heats of all the studied compounds (as well as the one reported for $\mathrm{TmNi_2B_2C}$) in terms of only two parameters, namely, an energy gap Δ and a characteristic temperature θ. The evolution of θ and Δ across the studied compounds correlates very well with the known magnetic properties. θ, as a measure of the effective Ruderman-Kittel-Kasuya-Yosida exchange couplings, scales reasonably well with the de Gennes factor. Δ, on the other hand, reflects predominately the anisotropic properties: ~2 K for $\mathrm{GdNi_2B_2C}$, ~6 K for $\mathrm{ErNi_2B_2C}$, ~7 K for $\mathrm{TbNi_2B_2C}$, and ~8 K for each of $\mathrm{HoNi_2B_2C}$ and $\mathrm{DyNi_2B_2C}$. The equality in Δ of $\mathrm{HoNi_2B_2C}$ and $\mathrm{DyNi_2B_2C}$, coupled with the similarity in their magnetic configurations, indicates that a variation of x in the solid solution $\mathrm{Ho}_x\mathrm{Dy}_{1-x}\mathrm{Ni_2B_2C}$ ($x<0.8$ and $T_c<T_N$) would not lead to any softening of Δ. This supports the hypothesis of Cho *et al.* (Ref. 35) concerning the influence of the collective magnetic excitations on the superconducting state. This work underlines the importance of spin-wave excitations for a valid description of low-temperature thermodynamics of borocarbides.

DOI: 10.1103/PhysRevB.67.224407 PACS number(s): 75.30.Ds, 75.30.Kz, 75.40.Cx, 74.70.Dd

I. INTRODUCTION

A wide variety of magnetic structures are manifested in $R\mathrm{Ni_2B_2C}$ series (see, e.g., Refs. 1 and 2 and Table I). These structures are stabilized by a fine balance of exchange, crystalline electric field (CEF), dipolar, and magnetoelastic forces. Under magnetic field or temperature variation, most of these structures undergo a cascade of phase transformations, yielding a rich variety of field-temperature (H-T) phase diagrams (see, e.g., Refs. 3–6). Interestingly, most of the zero-field magnetic ordered states of R=Tm, Er, Ho, Dy coexist with superconductivity, presenting model compounds wherein the interplay between superconductivity and magnetism can be investigated. Such investigations revealed that the superconductivity, though much influenced by, has a very weak influence on the prevailing magnetic order:[7] the energy gain due to the onset of magnetic order dominates by two order of magnitudes over that due to the onset of superconductivity.

The zero-field part of the H-T phase diagram of $\mathrm{HoNi_2B_2C}$ is particularly interesting: superconductivity sets-in at $T_c \simeq 8$ K. Just below this point, an incommensurate spiral state, $\vec{k}_c \simeq 0.92c^*$, develops (see, e.g., Refs. 1, 3, and 8). Furthermore, at ~6.3 K, an additional modulated state with $\vec{k}_a \simeq 0.55a^*$ emerges and around 5 K a deep minimum in H_{c2} develops.[9] At $T_N=5$ K, an orthorhombic lattice distortion[10] sets-in and, concomitantly, both the spiral and the a axis modulated states are replaced by a commensurate antiferromagnetic (AF) structure which coexists with superconductivity down to the lowest measurable temperatures. Generalized susceptibility calculation[11] related these modulated state to maxima in the exchange-coupling transform $J(k)$.

Remarkably, the magnetic ground structures of the heavy and magnetic $R\mathrm{Ni_2B_2C}$ compounds (see Table I) are particularly simple: in spite of the manifestation of an orthorhombic distortion and a liquid-helium-temperature magnetic modulation, their ground structures are either an equal-amplitude, AF-type squared-up state (as in R=Tm, Er, Tb, Gd) or an equal-amplitude, collinear, commensurate AF state (as in R=Ho, Dy). Then, it is of interest to investigate whether the low-temperature thermodynamics of these $R\mathrm{Ni_2B_2C}$ can be described in terms of small-amplitude spin-wave excitations and, in addition, to elucidate the character and dimensionality of these excitations. Such excitations can be probed by various techniques, among which is the magnetic specific heat. We carried out extensive zero-field specific-heat measurements on five single crystals $R\mathrm{Ni_2B_2C}$ (R=Er, Ho, Dy, Tb, Gd) covering at least the range 0.1 K$<T<T_N$. These specific heats, together with that of $\mathrm{TmNi_2B_2C}$ (Ref. 12), reveal a diversified and wide varieties of thermal evolutions. Nonetheless, based on a simple model, all of the specific-heat curves can be systematized in terms of only two parameters, namely, an effective exchange coupling and a magnetic anisotropy interaction.

The format of this paper is as follows: In Sec. II, we derive an approximate, but of wide applicability, expression for the magnon specific heat. Experimental techniques and

TABLE I. Some zero-field parameters of selected $R\mathrm{Ni_2B_2C}$ compounds. Superconducting T_c, magnetic T_N, *magnetic structure*, propagation *wave vector*, and *moment direction* are taken from Ref. 1. Squaring of the modulated SDW state is taken to occur at lower temperatures. The gap Δ and characteristic temperature θ were determined from the indicated equation and figure. θ_{exp} of $\mathrm{TmNi_2B_2C}$ is calculated by substituting into Eqs. (5) and (7) the fit values ($J_\perp = 0.8$ K and $|J_\parallel| = 0.2$) given by Movshvich *et al.*[12] θ_{deG} is the de Gennes scaling of θ taking that of $R=$Ho as a reference.

R	deG	T_c (K)	T_N (K)	Magnetic structure	Wave vector	Moment direction	Δ ± 0.2 K	θ_{exp} ± 0.2 K	θ_{deG} (K)	Equation number	Figure number
Gd	15.75	0	19.5	SDW	[.55,0,0]	[0,1,0]	1.9	12.5	34.0	6	1
Tb	10.5	0	15.4	SDW	[.555,0,0]	[1,0,0]	7	21.5	22.6	6	2
Dy	7.08	6	9.5	3D, AF	[0,0,1]	[1,1,0]	8.3	19.3	15.3	6	3
Ho	4.5	8	5	3D, AF	[0,0,1]	[1,1,0]	8.3	9.7	9.7	6	5
Er	2.5	10.5	5.9	SDW	[.553,0,0]	[0,1,0]	5.4	7.4	5.5	6	6
Tm	1.16	11	1.5	SDW	[.093,.093,0]	[0,0,1]	0	3.8	2.5	11	4 in Ref. 12

procedures are described in Sec. III. Results and their analysis are described in Sec. IV and discussed in Sec. V.

II. APPROXIMATE EXPRESSIONS FOR MAGNON SPECIFIC HEAT OF $R\mathrm{Ni_2B_2C}$

The magnetic structures of $R\mathrm{Ni_2B_2C}$ ($R=$Tm-Gd) can be visualized as magnetic layers that are stacked along the c axis.[1] The most dominant interactions are the Ruderman-Kittel-Kasuya-Yosida (RKKY) and anisotropic couplings. The former can be approximated by effective isotropic couplings, while the latter (a combination of dominant CEF, and weaker dipolar and anisotropic exchange forces) by an easy-axis anisotropy field $\vec{H}_a$:[13] this $\vec{H}_a$ representation is convenient for spin-wave calculation and is valid for the low-temperature phases of borocarbides. Considering the above-mentioned magnetic arrangement and the crystal symmetry, the magnetic couplings can be conveniently divided into two classes: J_{ij}^A that couples moments i and j within the same layer (denoted as A or B) and J_{ij}^{AB} that couples moments from different layers. Then at zero external field, the following Hamiltonian is expected to capture most of their low-temperature properties:

$$\mathcal{H} = -\sum_{\langle ij\rangle, L\in A,B} J_{ij}^L \vec{S}_i^L \cdot \vec{S}_j^L + \sum_{\langle ij\rangle A,B} J_{ij}^{AB} \vec{S}_i^A \cdot \vec{S}_j^B - g\mu_B \vec{H}_a \sum_{j\in A} \vec{S}_j^A + g\mu_B \vec{H}_a \cdot \sum_{j\in B} \vec{S}_j^B . \quad (1)$$

The first and second sum represent, respectively, interactions within the same layer and among different layers. The last two terms represent the anisotropic interactions. By standard spin-wave analysis, we obtained the following dispersion relation:

$$\hbar\omega_k = \sqrt{[SJ_\perp(0) - SJ_\perp(k) + SJ_\parallel(0) + g\mu_B H_a]^2 - [SJ_\parallel(k)]^2}, \quad (2)$$

where $J(k) = \Sigma J_{ij} \exp[ik(r_i - r_j)]\cdot$ $J_\parallel$ ($J_\perp$) represents the Fourier-transform parallel (perpendicular) to the c axis. The energy gap, $\Delta = \hbar\omega_{k=0}$, is

$$\Delta = \sqrt{(g\mu_B H_a)^2 + 2J_\parallel(0) g\mu_B S H_a}, \quad (3)$$

which defines an AF resonance frequency similar to the uniform mode of ordinary AF's.[13–16] Evidently, (i) Δ is zero whenever there is no anisotropy and (ii) Δ does not depend on the type nor on the strength of the intralayer coupling.

For evaluating the magnon specific heat, an explicit expression of $J(k)$ is required. In the absence of such an expression and for low-temerpature range, it is a common practice to assume a long-wave limit. Here, we restricted the expansion of $J(k)$ to the nearest neighbors only, leading to

$$\hbar\omega_k \approx \sqrt{\Delta^2 + C_x k_x^2 + C_y k_y^2 + C_z k_z^2}, \quad (4)$$

where C_x ($\approx C_y$ for weak orthorhombic distortion) and C_z are functions of the exchange couplings and geometrical factors (a and c are unit-cell parameters),

$$C_x = 16(J_\perp + J_\parallel) J_\parallel S^2 a^2 + 2J_\perp S(g\mu_B H_a) a^2,$$
$$C_z = 16 J_\parallel^2 S^2 c^2. \quad (5)$$

Then, the zero-field magnon specific heat is (rewritten so as to conform with the notation of Ref. 15)

$$C_M(T) = 3^{3/2} R(\Delta/\theta)^3 (\Delta/2T\pi^2) \sum_{m=1}^{\infty} [K_{Bessel}(2, m\Delta/T) + K_{Bessel}(4, m\Delta/T)], \quad (6)$$

where K_{Bessel} represents the modified Bessel function and

$$\theta = z|J_{eff}|S = \sqrt[3]{3^{3/2} 2(C_x C_y C_z)^{1/2}/(a^2 c)} \quad (7)$$

is a characteristic temperature, based on which $|J_{eff}|$ can be defined as being an effective exchange interaction that couples the magnetic moment to its z nearest neighbors.

For $T<\Delta$, Eq. (6) reduces to the exponential form

$$C_M(T) \simeq 2\frac{3^{3/2} R \Delta^{7/2}}{\pi^{3/2}\theta^3 T^{1/2}} \exp(-\Delta/T), \quad (8)$$

while for isotropic compounds or $T \gg \Delta$, it reduces to the high-temperature limit:[14,15]

$$C_M(T) \simeq \frac{3^{3/2} 4\pi^2}{15} R(T/\theta)^3. \quad (9)$$

TABLE II. List of values of γ, β, and θ of $R\mathrm{Ni_2B_2C}$ (R=Gd, Tb, Er, Ho, Dy, Tm). Also given are the expressions used for evaluating $C_s(T<T_c)$. The nuclear hyperfine parameters α and P (see Refs. 22) are also indicated: The upper (lower) values of $\mathrm{DyNi_2B_2C}$ correspond to the isotope ^{161}Dy (^{163}Dy). Data of $\mathrm{TmNi_2B_2C}$ were taken from Ref. 12.

R	γ (mJ/moleK^2)	C_s (J/moleK)	θ (β) K (mJ/moleK^4)	C_N α (K)	C_N P(K)	Figure number
Gd	17.5	γT	392 (0.1935)	0	0	1
Tb	17.5	γT	391 (0.196)	0.14(2)	0.02(1)	2
Dy	17.5	$3\gamma T^3/T_c^2$	388 (0.200)	$-.0396$ .0554	.009 .01	3
Ho	17.5	$3\gamma T^3/T_c^2$	386 (0.203)	0.29	.009	5
Er	17.5	$3\gamma T^3/T_c^2$	384 (0.206)	0.045	$-.0001$	6
Tm	$\sim$18	γT	$\sim$355 ($\sim$0.26)	0.0202	0	4 in Ref. 12

Equations (7) and (9) highlight the useful definition of $|J_{eff}|$.

A long-wave dispersion relation for an isotropic quasi-two-dimensional (2D) case can be derived from Eq. (4), if we set $C_z \ll C_x$ ($|J_\parallel| \ll J_\perp$) and $H_a=0$,

$$\hbar\omega_k \approx 8J_\parallel S + J_\perp S a^2(k_x^2+k_y^2). \tag{10}$$

Then, to lower order in $8J_\parallel S/T$, one obtains $C_M(T) = \pi RT/12SJ_\perp$ which reproduces the leading linear-in-T term in the expression reported by Movshovich *et al.*[12] who (starting from a quadratic dispersion relation and including correction for the 2D and the magnon-magnon interaction) obtained for the range $|J_\parallel|S<T<T_N$,

$$C_M(T) = (\pi R/12)(T/SJ_\perp - 6J_\parallel/\pi^2 J_\perp + 4J_\parallel S/3\pi^2 J_\perp T). \tag{11}$$

It is worth remarking that Eqs. (1–4) and (6) are of a more wide applicability than our above analysis might have suggested. Furthermore, a variety of limit expressions for the magnetic specific heat can be derived, depending on the relations among T and Δ [compare Eq. (6) with the limit equations (8), (9), and (11)]. Based on such a scheme, one is capable of rationalizing the vast variety of the low-temperature thermal evolution of thermodynamical quantities [such as $C_M(T)$] encountered in these (and any series similar to) borocarbides. It is reminded that this analysis is not adequate for the description of the contribution of the modulated states nor for the field-induced metamagnetic phases.

III. EXPERIMENTAL

Single crystals of $R\mathrm{Ni_2B_2C}$ (R=Er-Gd) were grown by floating-zone method.[17] Structural, magnetic, and transport characterizations are in agreement with published results. The temperature-dependent specific heat was measured on a semiadiabatic calorimeter (80 mK$<T<$25 K, precision better than 4%). The total specific-heat curves measured above 2 K are in agreement with the reported data.[8,18–20] However, we observed some discrepancy between the absolute values of $C_M(T)$ of single crystal and polycrystalline samples: though both specific heats were found to be given by approximately the same functional form, the absolute values of the fit parameters (θ and Δ) differ by as much as 40%.

For each compound, the total specific heat C_{tot} was analyzed as a sum of an electronic C_e (C_S when superconductivity is to be emphasized), a Debye C_D ($=\beta T^3$), a nuclear C_N, and a magnetic contribution C_M from the only magnetically active R sublattice. At temperatures of interest, C_e and C_D were estimated based on our specific-heat characterization[21] of single crystal $\mathrm{YNi_2B_2C}$ (γ=17.5 mJ/moleK^2 and β=0.12 mJ/moleK^4) which had been synthesized by the very same procedures as the one used for the other single crystals.

Within the superconducting region, C_S was evaluated as $3\gamma T^3/T_c^2$.[21] At any rate, for all the studied compounds, $C_M(T)$ is much larger than the sum of C_e and C_D. Consequently, even if C_e and C_D are taken as the bare values of $\mathrm{YNi_2B_2C}$, $C_M(T)$ would not be noticeably modified, ensuring that our conclusions would not be influenced.

$C_N(T)$ of $R\mathrm{Ni_2B_2C}$, when available, is of dominant importance only at very low temperatures and was evaluated by least-square fit using the appropriate hyperfine Hamiltonian; the obtained parameters (shown in Table II) compare favorably with those of the corresponding R metal[22] and $R\mathrm{Co_2B_2C}$ isomorphs.[23]

IV. RESULTS AND ANALYSIS

From the general feature of $C_M(T)$ curves (Figs. 1–3 and 5–6), one distinguishes four temperature regions: (i) a paramagnetic region, $T>T_N$, wherein $C_M(T)$ is predominantly due to a change in the population of the CEF levels, (ii) a critical region, $T\approx T_N$, wherein $C_M(T)$ is related to the critical fluctuations, (iii) an intermediate region wherein $C_M(T)$ reflects the magnetic character of the spiral/modulated states, and (iv) the low-temperature AF/squared-up states, of prime interest to this work, wherein the measured $C_M(T)$ is to be confronted with Eqs. (6) and (11) and therefrom θ and Δ are to be extracted.

Before we discuss the features of $C_M(T)$ for each compound, a word of caution is in order: just as in the case of R metals,[24] the propagation of errors due to successive subtraction of $C_e(T)$, $C_D(T)$, and $C_N(T)$ would eventually influence the absolute value of $C_M(T)$.

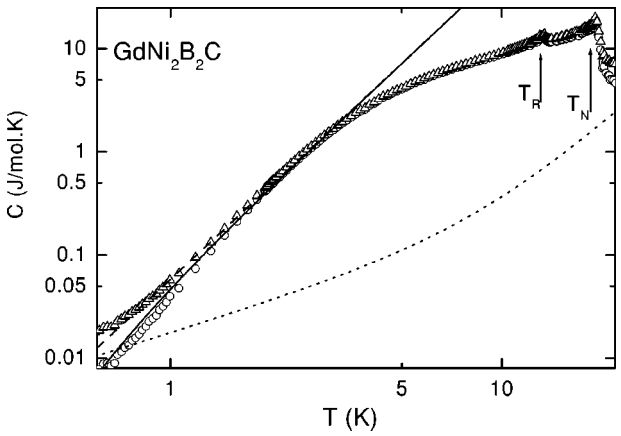

FIG. 1. Log-log plot of $C_{tot}(T)$ (triangles), $C_e(T)+C_D(T)$ (dotted), and $C_M(T)$ (circles) curves of single crystal $GdNi_2B_2C$. The solid line represents Eq. (6) with $\theta=12.5\pm0.2$ K and $\Delta=1.9\pm0.3$ K. For $\Delta<T<4$ K, $C_M(T)$ follows $0.058T^3$ J/moleK (dashed line) which is the high-T limit of Eq. (6) (see text).

A. $GdNi_2B_2C$

Below T_N, the zero-field magnetic structure[2] is a transverse sine-modulated type with $\vec{k}_a$ that changes from $0.551a^*$ at T_N to $0.550a^*$ at T_R, where a spin reorientation process sets-in. Below T_R, $\vec{k}_a$ reverts course and increases monotonically till it reach $0.553a^*$ at 3.5 K.

$C_M(T)$ of $GdNi_2B_2C$ (Fig. 1) reveals the onset of the magnetic order at $T_N=19.5$ K and the spin reorientation process at $T_R=13.5$ K, in agreement with earlier studies.[2,25–28] The thermal evolution of $C_M(T)$ within the amplitude-modulated state is distinctly different from that within the equal-amplitude, low-temperature state (see below). As mentioned above, within the modulated region the linearized spin-wave analysis is not applicable and one should resort to the findings of Schmitt and co-workers:[29] $C_M(T_N)$ of such a state suffers a strong reduction (almost 1/3) in comparison with the value (20.15 J/moleK) expected for an equal-amplitude AF state (our results are in excellent agreement with this statement).

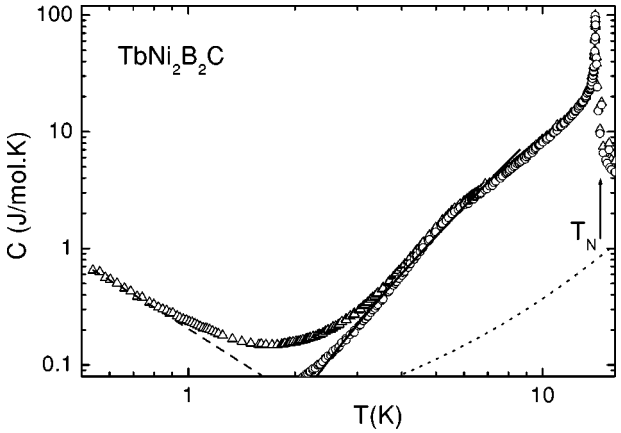

FIG. 2. Log-log plot of $C_{tot}(T)$ (triangle), $C_e(T)+C_D(T)$ (dotted), $C_N(T)$ (dashed) and $C_M(T)$ (circle) of single crystal $TbNi_2B_2C$. The solid line represents Eq. (6) with $\Delta=7.0\pm0.5$ K and $\theta=21.5\pm0.2$ K.

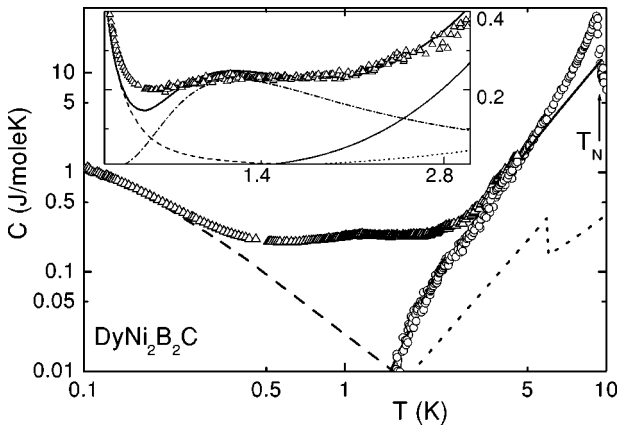

FIG. 3. A Log-log plot of $C_{tot}(T)$ (triangle), $C_e(T)+C_D(T)$ (dotted), $C_N(T)$ (dashed), and $C_M(T)$ (circles) of single crystal $DyNi_2B_2C$. The solid line represents Eq. (6) (see text). The inset shows the individual contribution of $C_{tot}(T)$ (symbol), $C_N(T)$ (dashed), the magnetic fit (lower solid line), $C_{sch}(T)$ [dash-dot, see Eq. (13)], and the upper solid line is the sum of all contribution.

On the other hand, Fig. 1 shows that for temperatures below 3.5 K, $C_M(T)$ follows faithfully Eq. (6) with $\theta=12.5\pm0.2$ K and $\Delta=1.9\pm0.3$ K. The numerical value of θ (for Δ see Sec. V) is physically acceptable as can be seen from the following arguments. First, the substitution of this θ into Eq. (7) yields $J_{eff}=0.58\pm0.2$ K, which is in close agreement with the value reported for $HoNi_2B_2C$ (Refs. 7, 30) and $TmNi_2B_2C$ (Ref. 12). Second, the substitution of θ into Eq. (9) predicts correctly the high-temperature limit, namely, $C_M(T>\Delta)=0.058T^3$ J/moleK (see Fig. 1). Third, the substitution of θ into the molecular-field relation,[14]

$$T_N=\tfrac{1}{3}\theta(S+1), \tag{12}$$

gives $T_N=18.8\pm0.3$ K which is in reasonable agreement with the experimentally determined value of T_N.

B. $TbNi_2B_2C$

A longitudinal spin-density wave (SDW), accompanied by an orthorhombic distortion, sets-in at T_N.[31,32] The magnitude of the modulation vector decreases from $0.551a^*$ near T_N to $0.545a^*$ at 2.3 K.[31] A weak ferromagnetic component develops below $T_{WF}\approx8$ K and at lower temperature a squaring up of the modulated state occurs.[31]

$C_M(T)$ of $TbNi_2B_2C$ (Fig. 2) shows the magnetic ordering at $T_N=14.5$ K and the WF-associated anomaly that peaks around 5.5 K. These features are in agreement with those reported by Tommy *et al.*[20] No attempt was made to analyze $C_M(T)$ within the amplitude-modulated state spanning the range $5\text{K}<T<T_N$. Below 5 K, where the orthorhombic-distorted squared-up state is expected, $C_M(T)$ follows convincingly the prediction of Eq. (6) with $\theta=21.5\pm0.2$ K and $\Delta=7.0\pm0.5$ K.

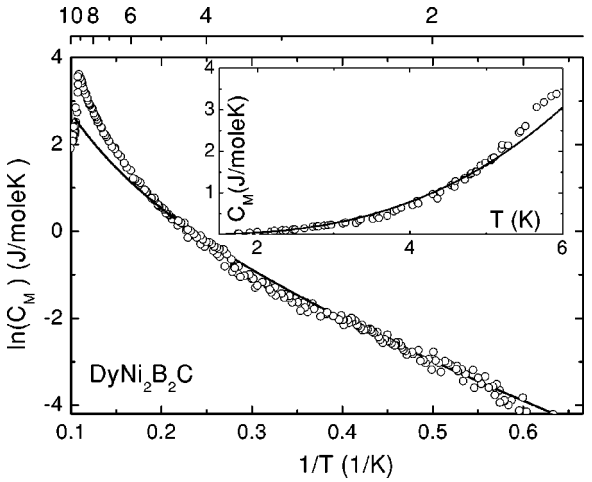

FIG. 4. $\ln(C_M(T))$ versus $1/T$ curve of single crystal $DyNi_2B_2C$. The data (circles) are compared to Eq. (6) (solid line) giving $\Delta = 8.3 \pm 0.3$ K and $\theta = 19.3 \pm 0.2$ K. The inset shows on a linear scale, $C_M(T)$ (circle) together with the comparison to Eq. (6) (see text).

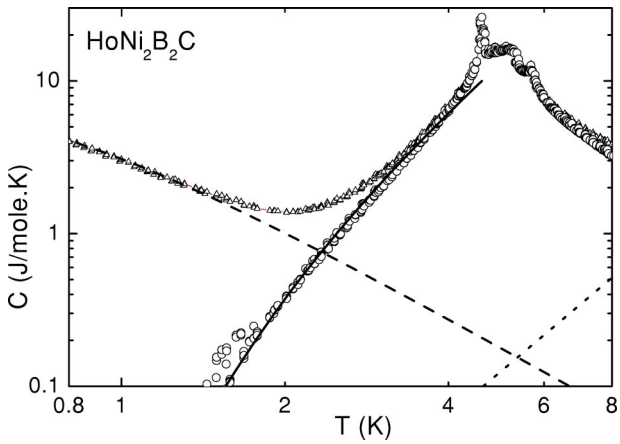

FIG. 5. A Log-log plot of $C(T)$ versus T of single crystal $HoNi_2B_2C$ showing $C_{tot}(T)$ (triangle), $C_e(T)+C_D(T)$ (dotted), $C_N(T)$ (dashed), and $C_M(T)$ (circle) contributions. The magnetic contribution (circles) are compared to Eq. (6) (solid line) giving $\Delta = 8.3 \pm 0.3$ K and $\theta = 9.7 \pm 0.2$ K (see text).

C. $DyNi_2B_2C$

This compound develops a commensurate AF structure below T_N with moments arranged in an identical manner as that of $HoNi_2B_2C$.[1,33] Moreover, superconductivity coexists with this AF order below $T_c \simeq 6$ K. In contrast to other Ni-based AF superconducting borocarbides, $DyNi_2B_2C$ presents the following distinct features: (i) no zero-field incommensurate or modulated state is evident.[1,33] However, for $T < 2$ K, anomalously large hysteresis and pronounced reentrant effects were observed for the field range 1 kOe$\leqslant H \leqslant$5.3 kOe[34] and (ii) the superconductivity emerges within a well developed AF order ($T_c < T_N$) and that T_c is extremely sensitive to nonmagnetic doping.[35]

$C_{tot}(T)$ (see Fig. 3) reveals the onset of the AF order at $T_N = 9.5 \pm 0.2$ K. Within the accuracy of our measurement, the superconducting jump at $T_c \simeq 6$ K is too small to be resolved. On carrying out the analysis of C_{tot} into its components (C_e, C_D, C_N, and C_M), we observed an additional contribution peaking at 1.2 K and having features reminiscent of a Schottky-like contribution. Accordingly, it was approximated by the standard two-level relation

$$C_{sch}(T) = R\left(\frac{\delta}{T}\right)^2 \exp\left(\frac{\delta}{T}\right) \Big/ \left[1+\exp\left(\frac{\delta}{T}\right)\right]^2, \qquad (13)$$

where δ is the energy separation. It was found out (see the inset of Fig. 3) that $\delta = 2.9$ K and that only 0.062 molar fraction is involved. Moreover, the fit is satisfactory for the high temperature tail but not so good at the lower-temperature part, suggesting that a multilevel Schottky contribution might be more appropriate. However, for the present discussion, the above two-level approximation is sufficient. It is highly possible that such a contribution is due to 6% defect/impurity which is on the limit of detection of our x-ray structural characterization. Coincidently, anomalous hysteresis effects were observed in the magnetostriction curves that were measured within the same temperature range.[34] At any case, for $T > \delta$, both $C_{sch}(T)$ and $C_N(T)$ are smaller than $C_M(T)$ (see inset of Fig. 3). Nevertheless, we considered $C_M(T) = C_{tot}(T) - C_S(T) - C_D(T) - C_N(T) - C_{sch}(T)$.

The thermal evolution of $C_M(T)$ is shown in a log-log plot in Fig. 3 and as $\ln[C_M(T)]$ versus $1/T$ plot in Fig. 4. In both figures, the comparison with Eq. (6) (solid line) is also presented. Evidently over a wide range of temperatures, $C_M(T \leqslant T_c)$ follows excellently Eq. (6) with $\theta = 19.3 \pm 0.2$ K and $\Delta = 8.3 \pm 0.3$ K.

D. $HoNi_2B_2C$

$C_{tot}(T)$ of single crystal $HoNi_2B_2C$ (shown in Fig. 5) reveals a cascade of three transitions that are usually attributed to magnetic transformations.[8,36] The signature of the onset of superconductivity is too weak to be observable in our present measurements. On the other hand, for $T < 5$ K, $C_M(T)$ follows the description of Eq. (6) with $\theta = 9.7 \pm 0.2$ K and $\Delta = 8.3 \pm 0.3$ K.

E. $ErNi_2B_2C$

Two intriguing features of the H-T phase diagram of $ErNi_2B_2C$ are[1,37–39]the onset of the incommensurate transversely polarized SDW state with $k_a = 0.553a^*$ at $T_N = 5.94$ K and the onset of weak ferromagnetism (WF) at $T_{WF} = 2.2$ K. These two events (none is able to quench superconductivity, $T_c = 10.5$ K) are well evident in $C_M(T)$ of Fig. 6. T_{WF}, in particular, is evident as a change of slope that separates two distinct thermal evolutions:[40] $C_M(T)$ within the amplitude-modulated state $T_{WF} < T < T_N$ and that within the squared-up state at $T < T_{WF}$. In the latter region, $C_M(T < T_{WF})$ is well described by Eq. (6) with $\theta = 7.4 \pm 0.2$ K and $\Delta = 5.4 \pm 0.3$ K.

F. $TmNi_2B_2C$

Superconductivity sets-in at 11 K and, below $T_N = 1.52 \pm 0.05$ K, coexists with a transversely polarized SDW state

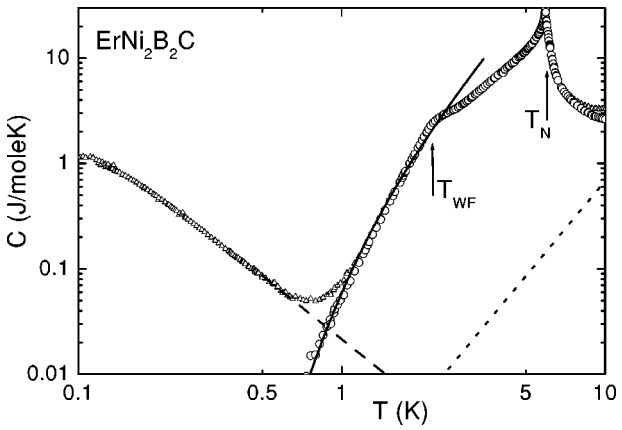

FIG. 6. A Log-log plot of $C_{tot}(T)$ (triangle), $C_e(T)+C_D(T)$ (dotted), $C_N(T)$ (dashed), and $C_M(T)$ (circle) of single crystal $ErNi_2B_2C$. The solid line is a comparison to Eq. (6) with $\theta=7.4\pm0.2$ K and $\Delta=5.4\pm0.3$ K (see text).

wherein the spins are pointing along the *c* axis and the modulation vector is (0.093,0.093,0).[1,12] At lower temperatures, the incommensurate SDW state squares up.[1] The magnetic specific heat of single crystal $TmNi_2B_2C$ was measured by Movshvich *et al.*[12] and was shown to follow Eq. (11) with $J_\perp\approx0.8$ K, $J_\parallel\approx0.2$ K.

V. DISCUSSION AND CONCLUSIONS

On a linearized spin-wave (noninteracting magnon gas) approach, one is limited to the low-temperature region of the ordered state which in the case of the borocarbides amounts to being restricted to below the liquid-helium temperatures. Within that temperature range, the model describes very successfully the magnetic contribution of the studied compounds indicating that C_M can be safely associated with the gapped collective excitations that propagate within the orthorhombic-distorted $3d$ AF (-type) structure.

The successful applicability of the model to the commensurate collinear AF ground structures of $R=$Ho, Dy is understandable. To justify its applicability to the cases of $R=$Tm, Er, Tb, Gd, it is sufficient to show that their ground structures are well squared up and that all the moments do have equal amplitudes and orient (or bunch) along a specific direction. The state of $ErNi_2B_2C$ below T_{WF} and that of $GdNi_2B_2C$ below 3.5 K provide the best illustrations of the fulfillment of this requirement. The collinear, equal amplitude, and squared-up character of the state of $ErNi_2B_2C$ below T_{WF} was elegantly revealed in the neutron-diffractions studies of Choi *et al.*[37] and Kawano-Furukawa *et al.*[38] It is remarked that the presence of weak ferromagnetism (reflected as kink that separate oppositely oriented domains) would hardly modify this picture since the excitation energy of the kink is much higher than that of the magnon.

A recent magnetoelastic study[41] on single crystal $GdNi_2B_2C$ demonstrated the presence of substantial magnetoelastic and anisotropic exchange interactions, in particular, below $T<T_R$. The magnitude of the ϵ^γ strain mode is very large and increases with decreasing temperature leading progressively to an orthorhombic-distorted magnetic state, wherein the moments, due to entropy arguments, approach equal amplitudes. Based on the suggestion of Detlefs *et al.*[2] the magnetic structure below T_R is either a transverse modulated state with moment orientation away from the *b* axis in the bc plane or a modified spirallike structure which, due to the low symmetry (2 mm) of the [100] direction, is likely to suffer fanning or bunching (becoming more stronger as the temperature is decreased). Tomala *et al.*,[26] on exploring these two structural possibilities, argued that the ^{155}Gd Mossbauer spectra at 4.2 K$<T<T_R$ were better fitted with a bunched spirallike state. Considering these and the above observations the low-temperature structure is either a *squared-up, equal-amplitude*, and collinear state or a strongly bunched and equal-amplitude state. As far as the magnon specific heat is concerned, the interactions in both structures can be represented by the Hamiltonian of Eq. (1).

Figs. 1–6 and Table I demonstrated convincingly that, based on only Δ and θ, the diverse functional form of the measured $C_M(T)$ can be systematized: when both Δ and θ are large, $C_M(T<\Delta)$ reflects a magnon contribution from an anisotropic magnetic structure as in $R=$Er, Ho, Dy, Tb. When Δ is relatively small but θ is large, $C_M(T>\Delta)$ reflects a magnetic contribution from a quasiisotropic magnetic structure as in $GdNi_2B_2C$. For a weak Δ and $J_\parallel$, $C_M(T)$ reflects a contribution from a quasi-$2D$ structure as in $TmNi_2B_2C$.

The evolution of Δ and θ across the studied compounds is reasonable. θ, on the one hand, reflects predominately the evolution of the de Gennes factor (see Eqs. (5) and (7) and Table I) as can be appreciated on observing that θ scales very well with the de Gennes factors for $R=$Tm, Er, Ho, Dy, Tb. That the experimentally determined θ of $GdNi_2B_2C$ is a factor of 3 lower than the one expected from de Gennes scaling may be attributed to the additional dependence of θ on H_a which for $GdNi_2B_2C$ is the lowest.

Δ, on the other hand, reflects the combined influence of the anisotropic forces and interlayer coupling. This is expressed by Eq. (3) which for the case of, say, $ErNi_2B_2C$ (considering $H_A\approx15$ kOe and $|J_\parallel|\approx0.1$ K) gives a value of 4 K which is close to the experimental value. The observation that Δ is nonzero for each of the studied compounds is in agreement with the reported anisotropic features of the magnetic and transport properties.[18] The strong anisotropy of each of $R=$Er, Ho, Dy, Tb is in accord with what is expected from their CEF properties. In contrast, the weak anisotropy observed in $GdNi_2B_2C$ is most probably due to a combination of anisotropic exchange and dipolar couplings.

It is interesting to discuss one particular aspect of the interaction between magnons and superconductivity in, say, $R=$Ho ($T_N<T_c$) and Dy ($T_c<T_N$). Noteworthy, the thermal evolution of $H_{c2}(T<T_N,T_c)$ of both $HoNi_2B_2C$ and $DyNi_2B_2C$ (Ref. 9) are very similar which, considering the above-mentioned similarity in their magnetic properties, suggests that the involved pair-breaking effects (in particular, the magnon-mediated one[42]) are similar. This, in turn, suggests that the magnon characteristic (say low-energy magnon spectra) in both compounds must be similar. This is indeed the case: the analysis of Secs. IV C and IVD showed that the energy cost for magnon excitation in both compounds is

practically equal ($\Delta \simeq 8$ K see Table I). Therefore, doping of Ho into $DyNi_2B_2C$ (up to 80% but still $T_c < T_N$) would not lead to a softening of Δ. Then, for this concentration range, there should be no variation in H_{c2} and T_c even though the de Gennes factor does vary. This provides an additional experimental confirmation of the hypothesis of Cho *et al.*[35] that the magnon spectrum of $(Dy_{1-x}Ho_x)Ni_2B_2C$ is hardly modified for $x < 0.8$. In contrast, for $(Dy_{1-x}Ho_x)Ni_2B_2C$ ($x > 0.8$), the onset of superconductivity occurs within the paramagnetic state and consequently the Dy dopant depresses T_c linearly as expected from the Abrikosov-Gorkov theory.

In summary, we were able to reveal the magnon specific-heat contribution of the heavy members of the borocarbides and to identify the expressions that describe their thermal evolution. These expressions (given in terms of only two physically accepted parameters) were derived from the spin-wave analysis of a simple Hamiltonian that consists of effective exchange couplings and anisotropic interactions. We investigated as well the influence of the magnons on the superconductivity of these AF superconductors.

Improvements and extension of this analysis are underway. These include, on the experimental side, probing the magnon contribution in single crystals of RNi_2B_2C by other (microscopic and macroscopic) techniques and, on the theoretical side, a better and more realistic approximation of $J(k)$, CEF effects, magnetoelastic, and anisotropic exchange forces.

ACKNOWLEDGMENTS

Partial financial support were provided by Brazilian agencies CNPq and FAPERJ.

[1] J.W. Lynn, S. Skanthakumar, Q. Huang, S.K. Sinha, Z. Hossain, L.C. Gupta, R. Nagarajan, and C. Godart, Phys. Rev. B **55**, 6584 (1997).
[2] C. Detlefs, A.I. Goldman, C. Stassis, P.C. Canfield, B.K. Cho, J.P. Hill, and D. Gibbs, Phys. Rev. B **53**, 6355 (1996).
[3] P.C. Canfield, S.L. Bud'ko, B.K. Cho, A. Lacerda, D. Farrell, E. Johnston-Halperin, V.A. Kalatsky, and V.L. Pokrovsky, Phys. Rev. B **55**, 970 (1997); A.J. Campbell, D.McK. Paul, and G.J. McIntyre, *ibid.* **61**, 5872 (2000).
[4] S.L. Bud'ko and P.C. Canfield, Phys. Rev. B **61**, 14 932 (2000); A.J. Campbell, D.McK. Paul, and G.J. MacIntyre, Solid State Commun. **115**, 213 (2000).
[5] C. Detlefs, F. Bourdarot, P. Burlet, P. Dervenagas, S.L. Bud'ko, and P.C. Canfield, Phys. Rev. B **61**, 14 916 (2000).
[6] P.C. Canfield and S.L. Bud'ko, J. Alloys Compd. **262-263**, 169 (1997).
[7] A. Amici, P. Thalmeier, and P. Fulde, Phys. Rev. Lett. **84**, 1800 (2000).
[8] P.C. Canfield, B.K. Cho, D.C. Johnston, Finnemore, and M.F. Hundley, Physica C **230**, 397 (1994).
[9] P.C. Canfield, P.L. Gammel, and D.J. Bishop, Phys. Today **51** (10), 40 (1998).
[10] A. Kreyssig, M. Loewenhaupt, J. Freudenberger, K.-H. Muller, and C. Ritter, J. Appl. Phys. **85**, 6058 (1999).
[11] Joo Yull Rhee, Xindong Wang, and B.N. Harmon, Phys. Rev. B **51**, 15 585 (1995).
[12] R. Movshovich, M.F. Hundley, J.D. Thompson, P.C. Canfield, B.K. Ch, and A.V. Chubkov, Physica C **227**, 381 (1994).
[13] C. Kittel, *Quantum Theory of Solids* (Wiley, New York, 1963).
[14] R. Kubo, Phys. Rev. **87**, 568 (1952).
[15] J.A. Eisele and F. Keffer, Phys. Rev. **96**, 929 (1954).
[16] L. R. Walker, in *Magnetism*, edited by G. T. Rado and H. Suhl (Acdemic Press, New York, 1963), Vol. 1, p. 299.
[17] H. Takeya, T. Hirano, and K. Kadowaki, Physica C **256**, 220 (1996).
[18] B.K. Cho, P.C. Canfield, L.L. Miller, D.C. Johnston, W.P. Beyermann, and A. Yatskar, Phys. Rev. B **52**, 3684 (1995).
[19] C.V. Tomy, M.R. Lees, L. Afalfiz, G. Balakrishnan, and D.McK. Paul, Phys. Rev. B **52**, 9186 (1995).
[20] C.V. Tomy, L.A. Afalfiz, M.R. Lees, J.M. Martin, D.McK. Paul, and D.T. Adroja, Phys. Rev. B **53**, 307 (1996).
[21] M. El Massalami, R.E. Rapp, and H. Takeya, in *Studies on High Temperature Superconductors*, edited by A. V. Narlikar (Novo Science, New York, in press).
[22] A.C. Anderson, B. Holmstrom, M. Kruis, and G.R. Pickett, Phys. Rev. **183**, 546 (1969); B. Holmstrom, A.C. Anderson, and M. Kruis, *ibid.* **188**, 888 (1969); M. Kruis, G.R. Pickett, and M.C. Veuro, Solid State Commun. **14**, 191 (1974).
[23] M. El Massalami, M.S. da Costa, R.E. Rapp, and F.A.B. Chaves, Phys. Rev. B **62**, 8942 (2000).
[24] B. Coqblin, *The Electronic Structure of Rare Earth Metals and Alloys: the Magnetic Heavy Rare Earths* (Academic Press, New York, 1977).
[25] P.C. Canfield, B.K. Cho, and D.C. Johnston, Physica B **215**, 337 (1996).
[26] K. Tomala, J.P. Sanchez, P. Vulliet, P.C. Canfield, Z. Drzazga, and A. Winiarska, Phys. Rev. B **58**, 8534 (1998).
[27] C. Godart, I. Felner, H. Michor, G. Hilscher, E. Tominez and E. Alleno, J. Alloys Compd. **275-277**, 642 (1998).
[28] M. El Massalami, B. Giordanengo, J. Mondragon, E.M. Baggio-Saitovitch, A. Takeuchi, J. Voirn, and A. Sulpice, J. Phys.: Condens. Matter **7**, 10 015 (1995).
[29] M. Bouvier, P. Lethuillier, and D. Schmitt, Phys. Rev. B **43**, 13137 (1991); J.A. Blanco, D. Gignoux, and D. Schmitt, *ibid.* **43**, 13145 (1991).
[30] B.K. Cho, B.N. Harmon, D.C. Johnston, and P.C. Canfield, Phys. Rev. B **53**, 2217 (1996).
[31] P. Dervenagas, J. Zarestky, C. Stassis, A.I. Goldman, P.C. Canfield, and B.K. Cho, Phys. Rev. B **53**, 8506 (1996).
[32] C. Song, J.C. Lang, C. Detlefs, A. Letoublon, W. Good, J. Kim, D. Wermeille, S.L. Budko, P.C. Canfield, and A.I. Goldman, Phys. Rev. B **64**, 020403 (2001); C. Song, D. Wermeille, A.I. Goldman, P.C. Canfield, J.Y. Rhee, and B.N. Harmon, *ibid.* **63**, 104507 (2001); C. Song, Z. Islam, L. Lottermoser, A.I. Goldman, P.C. Canfield, and C. Detlefs, *ibid.* **60**, 6223 (2001).
[33] P. Dervenagas, J. Zarestky, C. Stassis, A.I. Goldman, P.C. Canfield, and B.K. Cho, Physica B **212**, 1 (1995).

[34] Z.Q. Peng, K. Krug, and K. Winzer, Phys. Rev. B **57**, R8123 (1998).

[35] B.K. Cho, P.C. Canfield, and D.C. Johnston, Phys. Rev. Lett. **77**, 163 (1996).

[36] M. El-Hagary, M. Michor, C. Jambrich, R. Hauser, M. Gali, E. Bauer, and G. Hilscher, J. Magn. Magn. Mater. **177-181**, 551 (1995).

[37] S.-M. Choi, J.W. Lynn, D. Lopez, P.L. Gammel, P.C. Canfield, and S.L. Bud'ko, Phys. Rev. Lett. **87**, 107001 (2001).

[38] H. Kawano-Furukawa, H. Takeshita, M. Ochiai, T. Nagata, H. Yoshizawa, N. Furukawa, H. Takeya, and K. Kadowaki, Phys. Rev. B **65**, 180508 (2002).

[39] P.C. Canfield, S.L. Bud'ko, and B.K. Cho, Physica C **262**, 249 (1996).

[40] M. El Massalami, R.E. Rapp, E.F. Chagas, H. Takeya, J. Flores, and C.M. Chaves, J. Phys. Soc. Jpn. **71**, 582 (2002).

[41] M. El Massalami, H. Takeya, K. Hirata, M. Amara, R.-M. Galera, and D. Schmitt, Phys. Rev. B **67**, 144421 (2003).

[42] K. Levin, M. J. Nass, C. Ro, and G. S. Grest, in *Superconductivity in Magnetic and Exotic Materials*, edited by T. Matsubara and A. Kotani (Springer-Verlag, Berlin, 1963), p. 104; O. Fisher, in *Magnetic Superconductors*, edited by K. H. J. Buschow and E. P. Wohlfarth (Elsevier Science, Amsterdam, B.V., 1990), Chap. 6, p. 465.